

Fractal Active Shape Models

Polychronis Manousopoulos, Vassileios Drakopoulos, Theoharis Theoharis

Department of Informatics and Telecommunications,
University of Athens, Panepistimioupolis, 157 84, Athens, Greece.
{polyman, vasilios, theotheo}@di.uoa.gr

Abstract. Active Shape Models often require a considerable number of training samples and landmark points on each sample, in order to be efficient in practice. We introduce the Fractal Active Shape Models, an extension of Active Shape Models using fractal interpolation, in order to surmount these limitations. They require a considerably smaller number of landmark points to be determined and a smaller number of variables for describing a shape, especially for irregular ones. Moreover, they are shown to be efficient when few training samples are available.

1 Introduction

Active Shape Models (ASM, see e.g. [1]) are widely used for image segmentation and motion tracking; they have been proven to be efficient and robust in many areas of application, especially biomedical ones (see e.g. [2], [3], [4]). Extensions of the original ASM formulation have also been proposed, in order to increase their robustness, efficiency and applicability (see e.g. [5], [6], [7]).

In ASM applications, a significant number of *landmark points* has to be used in each *training sample* in order to model the desired variability of the allowable shape space, resulting in a time-consuming labelling process. Although (semi-)automatic methods have been developed for assisting this, the labelling remains a difficult and error-prone task. Moreover, the number of available training samples is often relatively small in practice, resulting in a rather restricted space of allowable shapes that reduces the efficiency of the image search.

Our motivation is to create an extension of the ASM that requires a considerably smaller number of landmark points, uses fewer variables to describe shapes, even irregular ones, thus increasing the accuracy of representation, and is efficient even for a small number of training samples. Motivated by the above points, we introduce the Fractal Active Shape Models, an extension of Active Shape Models using fractal interpolation.

2 Mathematical Background

2.1 Active Shape Models

Active shape models are statistical models of shape that can be applied to image search (see e.g. [1]). An ASM uses a *Point Distribution Model* (PDM) for the

statistical modelling of shapes in a given training set of sample images. This model is then used for locating statistically allowable shapes in other images.

A shape is described by a set of landmark points. These correspond to particular shape features and their interpretation should be consistent among all shapes of a class. For example, the boundary of the leaf *Laurus nobilis* depicted in Fig. 1(a) is represented by the 77 landmark points of Fig. 1(c). Moreover, they must be adequate for describing the shape variability of the training set as well as all other allowable shapes. The landmark points may be manually located on the training set images, but (semi-)automatic methods have also been developed, since this is often a time consuming process¹.

The sets of landmark points located in the training images are aligned in a common coordinate frame, e.g. using the iterative algorithm of [1]. An aligned shape can be represented by the vector

$$\mathbf{x} = (x_1, \dots, x_L, y_1, \dots, y_L), \quad (1)$$

where (x_i, y_i) , $i = 1, \dots, L$ are the aligned landmark points. The aligned shapes are then statistically modelled by applying Principal Component Analysis (PCA) to them; each shape \mathbf{x} is represented as

$$\mathbf{x} = \bar{\mathbf{x}} + \mathbf{P}\mathbf{b}, \quad (2)$$

where $\bar{\mathbf{x}}$ is the mean shape, \mathbf{P} is the matrix of eigenvectors of the covariance matrix of the shape vectors and \mathbf{b} is a vector of parameters determining the deviation of \mathbf{x} from the mean shape along each eigenvector. In practice, \mathbf{P} contains only the eigenvectors of the largest eigenvalues by eliminating insignificant eigenvectors that may correspond to noise in the training set. Equation (2) can be used for defining the space of allowable shapes by suitably constraining \mathbf{b} , e.g. $|b_k| \leq 3\sqrt{\lambda_k}$ for all elements b_k of \mathbf{b} , where λ_k is the eigenvalue of the corresponding eigenvector.

This statistical shape model of the training set can be used for locating similar shapes within graphical objects such as images. Starting with a rough approximation of the shape in the image, each point is moved to a nearby location to a better candidate. The points are usually moved along the shape boundary normal and are attracted to image edges or matching profiles of local intensity. This procedure is executed iteratively until it converges. At each step, the shape resulting from moving all points is constrained to the space of statistically allowable shapes. Therefore, the result is both compatible to the image structure as well as to the training set.

2.2 Fractal Interpolation

Fractal interpolation functions (see e.g. [8]) are based on the theory of *iterated function systems* (IFSs). An IFS, denoted by $\{X; w_n, n = 1, 2, \dots, N\}$, consists

¹ See Cootes T.F. and Taylor C.J., Statistical Models of Appearance for Computer Vision, <http://www.isbe.man.ac.uk/~bim>, March 2004, pp. 79–82 for a survey on landmark placement methods.

of a complete metric space (X, ρ) , e.g. $(\mathbb{R}^n, \|\cdot\|)$, and a finite set of continuous mappings $w_n: X \rightarrow X$, $n = 1, 2, \dots, N$. If w_n are contractions, then the IFS is termed *hyperbolic* and the transformation $W: \mathcal{H}(X) \rightarrow \mathcal{H}(X)$ with $W(B) = \bigcup_{n=1}^N w_n(B)$, where $\mathcal{H}(X)$ denotes the space of nonempty compact subsets of X , has a unique fixed point $A_\infty = W(A_\infty) = \lim_{n \rightarrow \infty} W^n(B)$, for every $B \in \mathcal{H}(X)$, which is called the *attractor* of the IFS.

Let us represent the given set of *data points* as $\{(u_m, v_m) \in \mathbb{R}^2: m = 0, 1, \dots, M\}$. In general, the interpolation is applied to a subset of them, the *interpolation points*, represented as $\{(x_i, y_i) \in \mathbb{R}^2: i = 0, 1, \dots, N\}$. Both sets are linearly ordered with respect to their abscissa, i.e. $u_0 < u_1 < \dots < u_M$ and $u_0 = x_0 < x_1 < \dots < x_N = u_M$. The interpolation points partition the set of data points into *interpolation intervals* and may be chosen equidistantly or not.

Let $\{\mathbb{R}^2; w_n, n = 1, 2, \dots, N\}$ be an IFS with affine transformations

$$w_n \begin{bmatrix} x \\ y \end{bmatrix} = \begin{bmatrix} a_n & 0 \\ c_n & s_n \end{bmatrix} \begin{bmatrix} x \\ y \end{bmatrix} + \begin{bmatrix} d_n \\ e_n \end{bmatrix}$$

constrained to satisfy

$$w_n \begin{bmatrix} x_0 \\ y_0 \end{bmatrix} = \begin{bmatrix} x_{n-1} \\ y_{n-1} \end{bmatrix} \quad \text{and} \quad w_n \begin{bmatrix} x_N \\ y_N \end{bmatrix} = \begin{bmatrix} x_n \\ y_n \end{bmatrix}$$

for every $n = 1, 2, \dots, N$. As results from solving the above equations (see e.g. [8], p. 213), the real numbers a_n, d_n, c_n, e_n are completely determined by the interpolation points, while the s_n are *free* parameters of the transformations satisfying $|s_n| < 1$, in order to guarantee that the IFS is hyperbolic with respect to an appropriate metric. The transformations w_n are *shear transformations* and the s_n their respective *vertical scaling* (or *contractivity*) factors.

It is well known (see for example [8]) that the attractor $G = \bigcup_{n=1}^N w_n(G)$ of the aforementioned IFS is the graph of a continuous function $f: [x_0, x_N] \rightarrow \mathbb{R}$ that interpolates the points (x_i, y_i) , $i = 0, 1, \dots, N$. This function is called *fractal interpolation function* (FIF) corresponding to these points and is self-affine.

If the interpolation points define a curve rather than a function, i.e. they are not linearly ordered with respect to their abscissa, then the direct use of a fractal interpolation function is not possible. In order to construct an IFS whose attractor interpolates the given points, and is therefore a curve, we can transform or extend the original points such that the application of a FIF is possible. This is then transformed or projected back to the plane to obtain a curve that interpolates the original points.

Curve fitting using fractal interpolation is discussed in [9], where the *Fractal Curve Fitting (FCF)* method is introduced. The latter will be used in this paper, since ASM are usually applied to objects with landmark points that define curves. The FCF method consists of transforming the data points $\{(u_m, v_m) \in \mathbb{R}^2: m = 0, 1, \dots, M\}$ by $T_1(u_m, v_m) = (u'_m, v'_m)$, $m = 0, 1, \dots, M$, where

$$u'_m = u_0 + \sum_{j=1}^m (|u_j - u_{j-1}| + \varepsilon) = u'_{m-1} + (|u_m - u_{m-1}| + \varepsilon),$$

$$v'_m = v_m,$$

and $\varepsilon > 0$ is an arbitrary constant necessary, when all data points in an interpolation interval have equal u -coordinates. A FIF is then constructed for (u'_m, v'_m) , $m = 0, 1, \dots, M$, and this is finally transformed by $T_2(u', v') = (u, v)$, where

$$u = u_{m-1} + (u_m - u_{m-1}) \left(\frac{u' - u'_{m-1}}{u'_m - u'_{m-1}} \right), \quad u' \in [u'_{m-1}, u'_m],$$

$$v = v',$$

resulting in a *fractal interpolation curve* that interpolates the initial points and passes near the remaining data points. The advantage of the FCF method over other methods is that it uses a smaller number of total affine transformation parameters (specifically half). Therefore, it is more suitable to our purpose as will become clearer in the next section.

3 Fractal Active Shape Models

We now introduce the *Fractal Active Shape Models (FASM)*, an extension of the ASM using fractal interpolation. Within the FASM framework, a shape is represented by a fractal interpolation curve rather than a set of landmark points. The interpolation points for constructing the curve need not be all the landmark points of the respective ASM, but only a relatively small subset of them. Indeed, using fewer interpolation points we are able to construct a curve that accurately describes the shape while requiring a smaller total number of variables.

Let us represent the set of all aligned shape boundary points, including the landmarks, extracted from the k -th training set image as $\{(u_m^k, v_m^k) \in \mathbb{R}^2: m = 0, 1, \dots, M\}$. The selected interpolation points, a subset of the landmark points, are represented accordingly as $\{(x_i^k, y_i^k) \in \mathbb{R}^2: i = 0, 1, \dots, N\}$. In the present work, the interpolation intervals are chosen with fixed length, i.e. every j -th data point is selected as interpolation point. A fractal interpolation curve is constructed for the shape points using the FCF method of Subsec. 2.2, with $\{\mathbb{R}^2; w_n^k, n = 1, 2, \dots, N\}$ being the respective IFS. The fractal interpolation curve, and therefore the respective shape, is described by the w_n^k transformation parameters, and is thus represented by the vector

$$\mathbf{f}_k = (a_1^k, \dots, a_N^k, c_1^k, \dots, c_N^k, s_1^k, \dots, s_N^k, d_1^k, \dots, d_N^k, e_1^k, \dots, e_N^k). \quad (3)$$

If the shape consists of multiple disjoint parts, e.g. a face, then we model each part with a fractal interpolation curve and create an aggregate vector \mathbf{f}_k of all transformation parameters for representing the shape. The parameters $a_n^k, c_n^k, d_n^k, e_n^k$ are determined by the interpolation points, while the parameters s_n^k by the remaining points. Thus, if we set $s_n^k = 0$ for every $n = 1, \dots, N$, resulting in piecewise linear interpolation, we are taking into account only the interpolation points, i.e. the FASM is equivalent to the respective ASM. Therefore, the FASM can be viewed as an extension of the ASM.

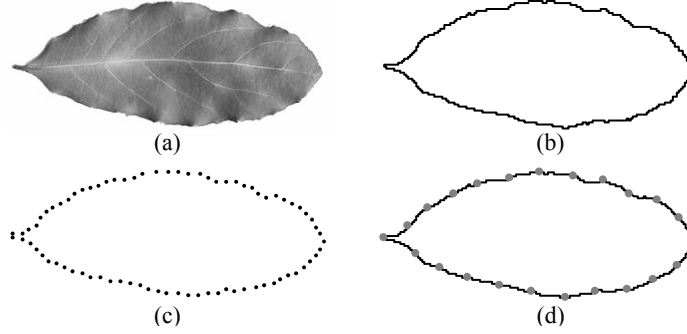


Fig. 1. (a) A leaf of *Laurus nobilis*. (b) The leaf's boundary consisting of 930 points. (c) The 77 landmark points representing the leaf. (d) The fractal interpolation curve of 23 interpolation points representing the leaf.

For example, the boundary of the leaf of *Laurus nobilis* depicted in Fig. 1(a) can be represented either by the 77 landmark points of Fig. 1(c), or by the fractal interpolation curve of 23 interpolation points of Fig. 1(d). The curve is constructed using the FCF method. The interpolation intervals have been chosen with fixed length and the vertical scaling factors s_n have been calculated with the analytic method of [10]. In both cases, the accuracy of representation is similar, but the FASM requires less than 30% of the landmark points of the ASM. Moreover, in the ASM the shape is represented by $154(= 2 \times 77)$ parameters, while in the FASM is represented by $115(= 5 \times 23)$ parameters², i.e. the FASM representation is more economical. This is because fractal interpolation exploits the presence of self-affinity in the data, thus allowing some degree of compression. The shape of this example is rather simple; for more complex and irregular shapes the FASM representation is expected to be even more profitable. This representation also has the advantage of describing the whole shape and not only a set of landmark points. Although the landmark points can capture the overall shape, the information of the remaining shape points is lost in the ASM. The FASM representation captures the whole shape using a smaller amount of data than the ASM.

The statistical modelling of the shapes is achieved by applying PCA to the vectors \mathbf{f}_k , $k = 1, \dots, K$. A shape can then be expressed as

$$\mathbf{f} = \bar{\mathbf{f}} + \mathbf{P}\mathbf{b}, \quad (4)$$

where $\bar{\mathbf{f}}$ represents the mean transformation, \mathbf{P} the matrix of eigenvectors of the covariance matrix of the shape vectors and \mathbf{b} the parameter vector. The space of allowable shapes is similarly defined by suitably constraining \mathbf{b} , e.g. $|b_k| \leq 3\sqrt{\lambda_k}$ for all elements b_k of \mathbf{b} , where λ_k is the eigenvalue of the corresponding eigenvector. Note that in the allowable shape space it should always be $|s_n| < 1$,

² An additional copy of the first point is automatically appended to the interpolation points in order to obtain a closed curve, thus resulting in 23 affine transformations.

for $n = 1, 2, \dots, N$. The feasibility of this approach stems from the fact that the attractor of an IFS, a fractal curve in our case, depends continuously on the affine transformation w_n^k parameters ([8], p. 111). Therefore it is reasonable to apply the aforementioned PCA.

In order to locate an allowable shape in an image, we use the following algorithm, which is an extension of the ASM algorithm:

1. Initialize an approximate fit to the given image.
2. Calculate the fractal interpolation curve for the current parameter vector \mathbf{b} and quantize it to pixel coordinates.
3. Move the curve points along the boundary normal towards the image edges. If duplicates exist, then remove them.
4. Calculate the parameter vector \mathbf{b}' for the adjusted points and limit it to the allowable space.
5. If the change in the shape is not negligible, goto Step 2.

The initialization in Step 1 of the algorithm can be done in various ways. For example, we may select a set of initial points as in the ASM case, calculate the respective affine transformation parameters $(a_n^k, c_n^k, d_n^k, e_n^k)$ and set the free parameters (s_n) to zero³. In Step 2, the number of calculated attractor points defines the balance between shape accuracy and execution time. Note that increasing the number of attractor points beyond a limit is unnecessary because of the quantization to pixel coordinates. In Step 3, the adjustment of the points is performed as in the original ASM algorithm; the image edges are calculated using a gradient operator, e.g. Sobel operator. In Step 4, the parameter vector, i.e. the IFS, for the adjusted points is calculated as before with the FCF method; the interpolation points are the adjusted interpolation points of the previous step.

4 Results

We have applied the FASM on a training sample consisting of eight images of leaves of *Laurus nobilis*, as the one depicted in Fig. 1. On each leaf, 23 landmark points have been placed and a fractal interpolation curve has been constructed for the whole leaf boundary using the FCF method. The vertical scaling factors of the affine transformations have been calculated using the analytic algorithm described in [10]. Each shape is represented by 115(= 5 × 23) parameters; an example is given in Fig. 2, where the 115 shape parameters are depicted in five groups. Examination of the shape vector in the form of these groups can reveal useful information about the shape. For example, we can conclude from the a_n and d_n groups that the interpolation intervals are similar in x -length, or, from the s_n group, that the leaf shape is most irregular, i.e. divergent from linear, in the first and eighth interval where the magnitude of s_n is the greatest.

The result of an image search example is depicted in Fig. 3. Specifically, the initial estimate of the shape is depicted in Fig. 3(a), while its final position after

³ The zero vertical scaling factors result in a piecewise linear attractor.

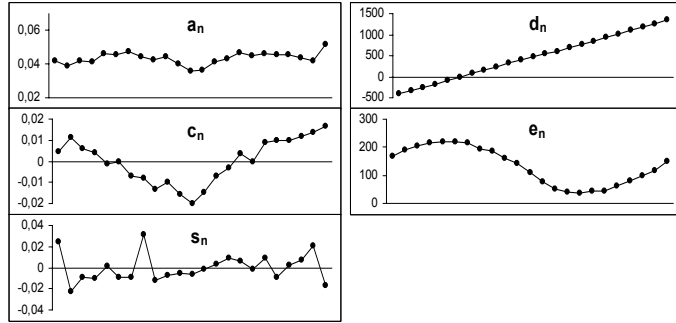


Fig. 2. The affine transformation parameters of the fractal interpolation curve of Fig. 1(d) divided into five groups, each consisting of 23 of the shape parameters.

convergence is depicted in Fig. 3(b). The leaf has been accurately detected in the image, with the FASM being able to capture its finer details with as few as 23 interpolation (i.e. landmark) points and 8 training samples.



Fig. 3. (a) The initial position of the shape in the image. (b) The final position of the shape after convergence.

5 Conclusions and Further Work

We have presented a novel extension of ASM that uses fractal interpolation for representing shapes. The proposed FASM have the advantage of requiring significantly fewer landmark points, even for irregular shapes, and of using fewer variables for representing a shape. Moreover, they are shown to be efficient, even when few training samples are available. Therefore, they are a competitive alternative to the original ASM, offering an efficient and practical approach. Future work will focus on extending the FASM to three dimensions and using piecewise self-affine fractal interpolation, which is expected to produce even better results.

Acknowledgements

This research project is co-financed by E.U.-European Social Fund (75%) and the Greek Ministry of Development-GSRT (25%), under the PENED programme 70/3/8405.

References

1. Cootes, T.F., Taylor, C.J., Cooper, D.H., Graham, J.: Active Shape Models - Their training and application. *Computer Vision and Image Understanding* **61** (1995) 38–59
2. Duta, N., Sonka, M.: Segmentation and interpretation of MR brain images: An improved Active Shape Model. *IEEE Transactions On Medical Imaging* **17** (1998) 1049–1062
3. Paragios, N., Jolly, M.P., Taron, M., Ramaraj, R.: Active Shape Models and segmentation of the left ventricle in echocardiography. In: *Scale Space and PDE Methods in Computer Vision, 5th International Conference, Lecture Notes in Computer Science*, Springer. (2005) 131–142
4. Smyth, P.P., Taylor, C.J., Adams, J.E.: Automatic measurement of vertebral shape using Active Shape Models. *Image and Vision Computing* **15** (1997) 575–581
5. Davatzikos, C., Tao, X., Shen, D.: Hierarchical Active Shape Models, using the wavelet transform. *IEEE Transactions On Medical Imaging* **22** (2003) 414–423
6. van Ginneken, B., Frangi, A.F., Staal, J.J., ter Haar Romeny, B.M., Viergever, M.A.: Active Shape Model segmentation with optimal features. *IEEE Transactions On Medical Imaging* **21** (2002) 924–933
7. Twining, C., Taylor, C.J.: Kernel principal component analysis and the construction of non-linear active Shape Models. In: *Proceedings of the British Machine Vision Conference*. (2001) 23–32
8. Barnsley, M.F.: *Fractals everywhere*. 2nd edn. Academic Press Professional, San Diego (1993)
9. Manousopoulos, P., Drakopoulos, V., Theoharis, T.: Curve fitting by fractal interpolation. submitted to the *Transactions on Computational Science*
10. Mazel, D.S., Hayes, M.H.: Using iterated function systems to model discrete sequences. *IEEE Trans. Signal Processing* **40** (1992) 1724–1734